

Alfvén Wave-Driven Proto-Neutron Star Winds And R-Process Nucleosynthesis

Takeru K. Suzuki¹ and Shigehiro Nagataki²

stakeru@scphys.kyoto-u.ac.jp

ABSTRACT

We propose magnetic proto-neutron star (PNS) winds driven by Alfvén waves as well as the neutrino heating as an appropriate site for the r-process nucleosynthesis. Alfvén waves excited by surface motions of a PNS propagate outwardly, and they heat and accelerate the wind by dissipation. Compared with the wind purely driven by the neutrino heating, larger entropy per baryon and shorter dynamical time scale are achieved, which favors the r-process. We study reasonable cases that a wave amplitude is 10% of Alfvén speed at the surface to find that a PNS with surface field strength, $\gtrsim 5 \times 10^{14}$ G, gives suitable wind properties for the r-process, provided that dissipation length of the wave is at most ~ 10 times of the PNS radius. We also compare properties of transcritical and subcritical winds in light of the r-process. We finally discuss possibilities of detections of γ -rays from radioactive nuclei and absorption lines due to Ba in supernova remnants which possess magnetars.

Subject headings: magnetic field – nuclear reactions, nucleosynthesis, abundances – plasmas – stars:neutron – supernovae:general – waves

1. Introduction

An origin of elements produced via rapid neutron capture process (r-process) still remains a mystery. It is one of the most important astrophysical problems to be solved. First, most massive nuclei (up to mass number, $A \simeq 250$) in the universe are synthesized through the r-process. It is not only scientifically interesting but also important to explore how, where, and when they are synthesized. Second, some r-process nuclei can be used as chronometers (Cowan et al. 1999; Wanajo et al. 2003). For example, the half-lives of ^{232}Th and ^{238}U are 1.405×10^{10} yr and 4.468×10^9 yr, respectively. We can estimate the ages of metal-poor astrophysical objects by their observed abundance ratio provided that the mass-spectrum of these produced r-process nuclei is predicted precisely. Third, chemical evolution of the r-process elements gives us a clue to reveal the history of the evolution of our Galaxy itself

(Ishimaru & Wanajo 1999; Tsujimoto, Shigeyama, & Yoshii 1999; Argast et al. 2004).

The conditions for the successful r-process nucleosynthesis are (Hoffman, Woosley, & Qian 1997; hereafter HWQ97): (i) high density, (ii) high entropy per baryon, (iii) short dynamical timescale, and (iv) small electron fraction, Y_e . This is because r-process nuclei are synthesized through the non-equilibrium process of the rapid neutron capture on seed nuclei, products as a consequence of the α -rich freezeout (HWQ97). In other words, an explosive, and neutron-rich site with high entropy is a promising candidate for the r-process nucleosynthesis.

The most probable sites, which possibly meet the above conditions, are collapse-driven supernovae (SNe; e.g., Woosley et al. 1994) and/or neutron star (NS) mergers (Freiburghaus et al. 1999; Rosswog et al. 2000). However, the collapse-driven SNe are thought to be more probable sites, because metal poor stars have already contained the r-process nuclei. Mcwilliam et al. (1995) reported that Eu, one of the r-process elements, is detected in 11 out of 33 metal-poor stars, which proves that r-process nuclei have been already produced at the very early stage in our

¹ Department of Physics, Kyoto University, Oiwake-cho Kitashirakawa Sakyo-ku, Kyoto 606-8502, Japan; JSPS Research Fellow

² Yukawa Institute for Theoretical Physics, Kyoto University, Oiwake-cho Kitashirakawa Sakyo-ku, Kyoto 606-8502, Japan

Galaxy. Comparing the event rate of collapse-driven SNe (10^{-2} yr $^{-1}$ Gal $^{-1}$; van den Bergh & Tammann 1991) with that of the NS merger (10^{-5} yr $^{-1}$ Gal $^{-1}$; van den Heuvel & Lorimer 1996; Bethe & Brown 1998), we can see that collapse-driven SNe are favored since they can supply the r-process nuclei at early epochs. Moreover, Cowan et al (1999) reported that the abundance ratio of r-process nuclei in metal poor stars are very similar to that in the solar system. This indicates that the r-process nuclei are synthesized through the similar conditions; most of the r-process nuclei are from a single candidate. So we assume in this paper that most of the r-process nuclei are synthesized in the collapse-driven SNe.

Many works have been done to uncover the nature of the r-process nucleosynthesis in the collapse-driven SNe so far. However, it seems quite difficult to produce the r-process elements compatible with the observations. Calculations of the neutrino-driven winds under the Newtonian gravity show that entropy per baryon is too small to succeed in the r-process (Takahashi et al. 1994; Qian & Woosley 1996; hereafter QW96). In order to solve this difficulty, QW96 further included a post-Newtonian correction to the gravitational force. Cardall and Fuller (1997) extended QW96 by considering a fully general relativistic treatment. Both showed that the relativistic effects favored the r-process nucleosynthesis. After an extensive survey of the general relativistic effects, Otsuki et al. (2000) gave a quantitative conclusion that the r-process was realized in the strong neutrino-driven winds ($L_\nu \sim 10^{52}$ erg s $^{-1}$) as long as a massive ($\sim 2.0 M_\odot$) and compact (~ 10 km) proto-NS (PNS) is formed. This is finally confirmed by Sumiyoshi et al. (2000), Wanajo et al. (2001), and Thompson, Burrows, & Meyer (2001). Although it is very intriguing as the solution is firstly discovered by the introduction of the relativistic effects, the above conditions can be satisfied only by a soft equation of state (EOS) based on a few nonstandard models for sufficiently cold nuclear matter (Wiringa, Fiks, & Fabrocini 1988). In fact, the r-process nuclei can not be produced in the numerical simulations with a normal EOS (Sumiyoshi et al. 2000). Thus it seems that the difficulty can not be solved completely by the effects of the general relativity only.

There is only one report of the successful nucleosynthesis (Woosley et al. 1994). In their numerical simulation, the entropy per baryon becomes high enough to produce the r-process nuclei successfully at

very late phase of the neutrino-driven wind (~ 10 s after the core-collapse). However, such high entropy is inconsistent with a reliable analytical formulation based on the Newtonian gravity (QW96). The general relativistic effects, taken into account in Woosley et al. (1994), cannot explain the discrepancy, either (Otsuki et al. 2000). Furthermore, nuclei with $A \sim 90$ are overproduced, which is incompatible with the solar system abundances. The successful mass-spectrum at the late phase would also be destroyed by neutral-current neutrino spallations of nucleons from ^4He (Meyer 1995). Although the result of Woosley et al. (1994) is remarkable, it would not be concluded that the problem is settled completely.

Facing such difficulties, it is worth exploring additional effects that encourage the r-process nucleosynthesis. It is argued that the wind properties are improved to be suitable for the r-process by a small increase of energy input at a few tens kilometers above the surface, which may be operated by wave mechanism and/or magnetic activities (QW96; Thompson et al. 2001). Recent observations show that some fraction of NSs has relatively strong magnetic field, $B \gtrsim 10^{14}$ G (e.g. Guseinov, Yazgan, & Ankay 2003). It is expected to effect dynamics and energetics of the neutrino-driven winds because the magnetic pressure becomes comparable to or even larger than the thermal pressure (Thompson 2003). As a result, abundances of the r-process products would be different in the winds from such magnetic PNSs. Let us introduce previous works dealing with the effects of magnetic field around the PNSs. Nagataki (2001) pointed out importance of the magnetic field and investigated a steady, subsonic, and rigidly rotating jet, although the r-process conditions can not be satisfied in the winds. Nagataki and Kohri (2001) further examined a steady and subsonic wind by using magneto-rotational wind solutions (Weber & Davis 1967), although they only explored field strengths, 5×10^{11} G, which is not dynamically important because of the complicated critical point topologies encountered in the steady state solution. As a result, they found that the wind properties are still inappropriate for the r-process nucleosynthesis. Thompson (2003) considered an ordered dipole with larger field strength up to 10^{16} G and pointed out an importance of trapping of the plasma heated by the neutrino. He estimated enhancement of the entropy due to the trapping to conclude that the ordered dipoles with surface fields of $> 6 \times 10^{14}$ G give the suitable circumstances for the r-process nucleosynthesis.

We propose another mechanism operated by magnetic fields. Alfvén waves are supposed to play a role in heating and accelerating astrophysical plasma. In particular those generated by surface convective motions are reliable sources in the solar corona and wind. As the waves have momentum and energy, their dissipation leads to acceleration and heating of the surrounding plasma (e.g. Belcher 1971; Suzuki 2004). Excitation of Alfvén waves is also introduced in NSs with strong magnetic field (Thompson & Duncan 1996). Then, those Alfvén waves will contribute to the heating and acceleration in the magnetosphere, similarly to the solar corona. To date, however, a role of these waves in PNS winds has not been studied. Then, we investigate effects of the Alfvén waves on the physical conditions such as the entropy per baryon and the dynamical timescale, and we discuss whether they can help the synthesis of r-process nuclei.

In section 2, we explain the formulation for Alfvén wave-driven PNS winds in the hot bubble. In section 3, we show the results. Discussions and Conclusion are presented in section 4 and 5.

2. Methods

2.1. Formulations

We present formula for the PNS winds in existence of the Alfvén waves which excited at the surface. Although this is not addressed in this paper, excitation of Alfvén waves is studied in NSs with strong magnetic field by several authors (Thompson & Duncan 1996; Thompson, Lyutikov, & Kulkarni 2002; Kojima & Okita 2004). A certain fraction of magnetic energy in the core of a NS is transferred to seismic waves in the crust. Such waves will be coupled with Alfvén waves in the magnetosphere (Blaes et al. 1989). In other words, Alfvén waves would be excited from around the surface. Moreover, the PNS is convectively unstable (Epstein 1979). Driven turbulent-like motions (Keil, Janka, & Müller 1996) will further contribute to the excitation of the Alfvén waves.

We consider one-dimensional magnetic flux tube which is radially open. Alfvén waves excited with amplitude of magnetic field, δB_0 , at the PNS surface propagate outwardly along with this field line. The plasma also flows along it when the ideal MHD condition is satisfied. Then, it can be assumed that all the physical variables depend only on radial distance, r . We also assume steady state with continuous injection of the Alfvén waves from the surface. We do not con-

sider effects of the rotation of a PNS and the general relativity to focus on a role of Alfvén waves in this paper.

Conservation of magnetic flux, $\nabla \cdot \mathbf{B} = 0$, gives

$$Br^2 = B_0 r_0^2 = \text{const}, \quad (1)$$

where B is radial field strength and B_0 is field strength at the PNS surface, $r = r_0$. Mass conservation under the steady state condition becomes

$$4\pi r^2 \rho v = \text{const}, \quad (2)$$

where ρ is density and v is velocity. Momentum conservation is expressed as

$$v \frac{dv}{dr} = -\frac{GM}{r^2} - \frac{1}{\rho} \frac{dP}{dr} - \frac{1}{\rho} \frac{dP_w}{dr}, \quad (3)$$

where M is mass of the PNS and P is total pressure of nonrelativistic matter, relativistic particles, and photon radiation (QW96). P_w is wave pressure which can be written as a function of wave amplitude in magnetic field, δB , as $P_w = \frac{\delta B^2}{16\pi}$ (Lamers & Cassinelli 1999). An equation for internal energy, \mathcal{E} , is

$$\dot{q}_\nu + \dot{q}_w = v \left(\frac{d\mathcal{E}}{dr} - \frac{P}{\rho^2} \frac{d\rho}{dr} \right), \quad (4)$$

where \dot{q}_ν denotes neutrino heating and \dot{q}_w is heating due to dissipation of the Alfvén waves.

In this study, we consider three processes with respect to neutrino heating and cooling, that is, neutrino scattering processes on electrons and positrons, neutrino absorption on free nucleons, and electron and positron capture on free nucleons. \dot{q}_ν can be calculated as a function of neutrino luminosity, L_ν , and energy, ϵ_ν , following Tubbs & Schramm (1975), Goodman, Dar, & Nussinov (1987), and QW96. We do not consider heating from neutrino/anti-neutrino annihilation and cooling from electron/positron annihilation which are taken into account in QW96, because they are not effective as shown by Otsuki et al. (2000). We set $\dot{q}_\nu=0$ for $T \leq 0.5$ MeV, because free nucleons are bound into α -particles and heavier nuclei and electron-positron pairs annihilate into photons.

The wave heating, $\dot{q}_w (> 0)$, satisfies an equation describing variation of wave energy:

$$-\rho \dot{q}_w = \nabla \cdot \mathbf{F}_w - v \frac{dP_w}{dr} \equiv \frac{v_A}{v_A + v} \nabla \cdot \mathbf{H}_w, \quad (5)$$

where $v_A = B/\sqrt{4\pi\rho}$ is Alfvén speed and $\mathbf{F}_w = \frac{\delta B^2}{8\pi} (\mathbf{v}_A + \frac{3}{2}\mathbf{v})$ is wave energy flux (Jacques 1977).

H_w is wave action constant which is expresses as (Jacques 1977)

$$H_w \equiv \frac{\delta B^2}{8\pi} \frac{(v_A + v)(v_A + v)}{v_A}, \quad (6)$$

which is a conserved quantity in moving media if the wave does not dissipate. Physical meaning of eq.(5) is quite similar to the 1st law of thermodynamics; variation of wave energy flux, $\nabla \cdot \mathbf{F}_w$, is determined by work done by wave, $-v \frac{dP_w}{dr}$, and wave dissipation, $-\rho \dot{q}_w$. Alfvén wave pressure gradient is written as a function of \dot{q}_w as (Lamers & Cassinelli 1999)

$$\frac{1}{\rho} \frac{dP_w}{dr} = -\frac{\dot{q}_w}{2(v + v_A)} + \frac{\delta B^2}{32\pi\rho} \frac{3v + v_A}{v + v_A} \frac{1}{\rho} \frac{d\rho}{dr} \quad (7)$$

Alfvén waves are supposed to hardly dissipate due to the uncompressional character, if they travel in uniform media. However, amplitude of those propagating in the stratified plasma, such as atmosphere of stellar objects, is amplified so that non-linear damping processes becomes important. Ingoing Alfvén waves are excited by parametric decay instability, coupling between the outgoing waves and density fluctuations (Goldstein 1978). These ingoing Alfvén waves interact with the pre-existing outgoing waves to lead to turbulent-like cascade and subsequent wave dissipation. The parametric decay also generates sound waves, which easily dissipate due to their compressive character. Linearly polarized waves dissipate through formation of fast MHD shocks in magnetically dominated plasma as a consequence of nonlinear steepening of the wave fronts (Hollweg 1982; Suzuki 2004). Transverse gradient of Alfvén speed leads to resistive and viscous dissipation due to phase mixing of Alfvén waves traveling along neighboring field lines (Heyvaerts & Priest 1983). Kinetic effects, such as ioncyclotron resonance, might work in the dissipation (e.g. Cranmer, Field, & Kohl 1999). Observation in the solar corona shows an evidence of dissipation of Alfvén waves in a region closed to the surface (Doyle, Teriaca, & Banerjee 1999). Therefore, Alfvén waves, if they exist, are also expected to dissipate in the PNS winds, though the dissipation mechanisms are quite complicated as discussed above. In this paper, we adopt a simple parameterization for the wave damping by using a dissipation length, l ,

$$H_w = \frac{r_0^2}{r^2} H_{w,0} \exp\left(\frac{r_0 - r}{l}\right), \quad (8)$$

where $H_{w,0}$ is wave action at the PNS surface, $r = r_0$. Equations (5) and (8) give an explicit form of heating function as

$$\dot{q}_w = \frac{1}{\rho} \frac{v_A}{v + v_A} H_{w,0} \frac{r_0^2}{r^2} \frac{\exp(\frac{r_0 - r}{l})}{l} \quad (9)$$

Once initial wave energy flux, $F_{w,0}$ ($\simeq H_{w,0}$ for $v \ll v_A$), is fixed, l controls distribution of energy and momentum transferred from the waves; heating and acceleration occurs in inner regions for cases with smaller l , and vice versa.

Let us give a rough estimate of l based on analogy to the nonlinear damping of Alfvén waves in the solar corona. Generally, l is expected to have a linear dependence on wave length, $\lambda = v_A \tau$, where τ is wave period:

$$l = f \lambda,$$

where f is a proportional coefficient which is expected to have a negative dependence on $\delta B/B$ for the nonlinear damping. Suzuki (2004) considered Alfvén wave with $\lambda \sim 10^5$ km ($v_A \sim 1000$ km/s and $\tau \sim 100$ s) as a typical one in the solar corona. He studied dissipation by fast shocks, one of the nonlinear mechanisms, to find that l becomes an order of R_\odot for $\delta B/B \simeq 0.2 - 0.3$, where $R_\odot = 7 \times 10^5$ km is the solar radius. This shows $f \sim 10$, which means that the Alfvén waves dissipate typically by 10 times of λ . In PNS winds, timescale for convections can be regarded as one of the typical wave periods. Hydrodynamical simulations show that convective cells with several kilometers move with velocity $10^3 - 10^4$ km/s (Keil et al. 1996), which gives $\tau \sim 1$ ms. We consider $B_0 \gtrsim 10^{14}$ G for Alfvén wave-driven winds, which corresponds to $v_A \sim 10^4$ km/s. Then, typical wave length becomes $\lambda = v_A \tau \sim 10$ km ($= r_0$). If the amplitude is similar to that in the solar wind, the similar f (~ 10) may arise. It follows that we can assume $l \sim 10r_0$ as a fiducial value. However, l would vary a lot if waves with different τ dominantly worked. Therefore, we consider three cases, $l = (5, 10, 30) \times r_0$ in this paper.

2.2. Numerical Integration

We describe a practical method to determine the wind structures for various inputs of Alfvén waves. Adopted parameters for a PNS and the input neutrinos are summarized in tab.1. We set the density at the inner boundary to be 10^{10} g/cm³, following the result of Wilson's numerical simulation in Woosley et

al. (1994) (see also Otsuki et al. 2000). Temperature at the surface is derived from energy balance between the neutrino heating and cooling, following QW96:

$$T_0 = 1.19 \times 10^{10} \left[1 + \frac{L_{\nu_e}}{L_{\bar{\nu}_e}} \left(\frac{\epsilon_{\nu_e, \text{MeV}}}{\epsilon_{\bar{\nu}_e, \text{MeV}}} \right)^2 \right]^{\frac{1}{6}} L_{\nu_e, 51}^{\frac{1}{6}} R_6^{-\frac{1}{3}} \epsilon_{\nu_e, \text{MeV}}^{\frac{1}{3}} \quad [K], \quad (10)$$

where $L_{\nu, 51}$ is the individual neutrino luminosity in 10^{51} ergs s^{-1} , R_6 is the neutron star radius in 10^6 cm ($= 10$ km), $\Delta = 1.293$ MeV is the neutron-proton mass difference, and $\epsilon_{\nu, \text{MeV}}$ is a neutrino energy in MeV. We assume that the neutron star radius is equal to the neutrino sphere radius.

Amplitude of Alfvén waves is set to be $\delta B_0/B_0 = 0.1$ at the surface, although it is quite uncertain. $\delta B_0/B_0 = 0.1$ indicates that velocity amplitude is 10% of the phase speed (Alfvén speed in this case), which is often seen in astrophysical objects; for example, at the solar surface speed of the convective motions (~ 1 km/s) is $\sim 10\%$ of the sound speed (~ 10 km/s). By the assumption of the constant $\delta B_0/B_0$ the input wave energy flux, $F_{w,0} \simeq H_{w,0}$, is proportional to B_0^3 (note that $v_{A,0} \propto B_0$).

Integration starts from the surface for an initial guess of velocity, v_0 . Temperature is integrated according to eq.(4). Background magnetic field, B , is fixed by the conservation of magnetic flux (eq.(1)). δB is determined in order to satisfy the dissipation model of Alfvén wave (eq.(8)). We integrate velocity by an equation, transformed from the momentum equation (3) with help of eq.(7),

$$\frac{1}{v} \frac{dv}{dr} = \left[\frac{1}{r} (2v_s^2 + 2w^2 - \frac{GM}{r}) - \frac{\dot{q}_\nu + \dot{q}_w}{3v} + \frac{\dot{q}_w}{2(v + v_A)} \right] \left[v^2 - v_s^2 - w^2 \right]^{-1}, \quad (11)$$

where $v_s = (\frac{4}{3} \frac{P}{\rho})^{1/2}$ is adiabatic sound speed and

$$w \equiv \sqrt{\frac{\delta B^2}{32\pi\rho} \frac{3v + v_A}{v + v_A}}.$$

is a variable in unit of velocity, indicating contribution of the Alfvén waves. When deriving eq.(11) from eq.(3), we have assumed that pressure by relativistic electrons and positrons and photon radiation dominates the other components, and the degeneracy is negligible, namely,

$$P \simeq \frac{11}{4} \frac{aT^4}{3}, \quad (12)$$

where $a (= 7.56 \times 10^{-15} \text{ erg cm}^{-3} \text{ K}^{-4})$ is a Stefan Boltzmann radiation constant. The above assumption is applicable only for $T \gtrsim 0.5$ MeV because otherwise the electron-positron pairs annihilate and the remained electrons become nonrelativistic. Although the effect of the pair annihilation gives a modification of eq.(12) by a factor of $(11/4)^{1/3}$, this seems to influence on the dynamics quite little (Sumiyoshi et al. (2000)). Contribution of the non-relativistic gas to the pressure is also small for $T \gtrsim 0.1$ MeV in our Alfvén wave-driven winds. This is because density in the Alfvén wave-driven winds is smaller than the neutrino driven-winds on account of rapid acceleration. Once v is determined by eq.(11), ρ is derived from the mass conservation equation (2).

For the velocity structure we both consider transcritical and subcritical solutions. When deriving transcritical solutions, a critical point is derived from the condition that both numerator and denominator of eq.(11) are zero. Then, we iteratively determine an initial guess of v_0 to smoothly pass through the critical point by a shooting method. On the other hand, subcritical solutions cannot be uniquely determined. We derive subcritical solutions for given mass flux by reducing v_0 from the transcritical values.

We have checked an accuracy of the integration by monitoring whether how precisely a Bernoulli equation shown below is fulfilled as a function of r :

$$\left[\frac{v^2}{2} + \frac{TS}{m_N} - \frac{GM}{r} + \frac{F_W}{\rho v} \right]_{r_0}^r = \int_{r_0}^r dr \frac{\dot{q}_\nu}{v}, \quad (13)$$

where m_N is the nucleon rest mass and $S = m_N \frac{4P}{\rho}$ is entropy per baryon (for non-degenerate and relativistic gas). We have found that our numerical integration satisfies the above equation at least within 3% which is acceptable for the purpose of our model calculations.

Table 1: Adopted Parameters. r_0 is PNS radius, ρ_0 is surface density, and M is PNS mass in unit of solar mass, M_\odot . L_ν is neutrino luminosity per flavor and ϵ_ν is neutrino energy.

r_0	10km
ρ_0	$10^{10} \text{ g cm}^{-3}$
M	$1.4 M_\odot$
L_ν	$10^{51} \text{ erg s}^{-1}$
ϵ_{ν_e}	12 MeV
$\epsilon_{\bar{\nu}_e}$	22 MeV
$\epsilon_{\nu_\tau}, \epsilon_{\bar{\nu}_\tau}, \epsilon_{\nu_\tau}, \epsilon_{\bar{\nu}_\tau}$	34 MeV

2.3. Condition for Entropy

When we discuss whether r-process nucleosynthesis can occur or not, we use a criterion given by HWQ97, which is written as

$$S \gtrsim 2 \times 10^3 Y_e \left(\frac{t_{\text{exp}}}{s} \right)^{1/3} \quad (14)$$

for $Y_e \geq 0.38$, where S is measured in unit of Boltzmann constant, k_B , and t_{exp} is expansion time scale defined as time elapsed from $T = 9 \times 10^9 \text{ K}$ to $T = 2.5 \times 10^9 \text{ K}$. This is the condition for production of the r-process nuclei with mass number $A \sim 200$ (QW96).

Electron fraction Y_e at the time when α -rich freeze-out takes place can be estimated as (QW96)

$$Y_e = \left(1 + \frac{L_{\bar{\nu}_e} \epsilon_{\bar{\nu}_e, \text{MeV}} - 2\Delta + 1.2\Delta^2/\epsilon_{\bar{\nu}_e, \text{MeV}}}{L_{\nu_e} \epsilon_{\nu_e, \text{MeV}} + 2\Delta + 1.2\Delta^2/\epsilon_{\nu_e, \text{MeV}}} \right)^{-1}. \quad (15)$$

When we substitute the parameters shown in tab.1, we estimate $Y_e = 0.43$, at which the r-process criterion (eq.(14)) is applicable. In realistic situations, L_ν and ϵ_ν may vary, hence, we consider cases with $Y_e = 0.4 - 0.5$

3. Results

In this section, we examine how the dissipation of the Alfvén waves modifies the wind structures. In particular we discuss possibilities of the r-process nucleosynthesis in light of the criterion, eq.(14), for S and t_{exp} .

The transcritical solutions are generally stable if sufficient energy injection is given and the winds blow into free space. In the PNS winds, however, ejected shells exist in the outer region and interaction between the shells and winds leads to formation of termination shock. We expect the flow stays transcritical if a position of the shock is far outside of the critical point. Otherwise, the shock works as an outer boundary so that the flow might become subcritical eventually. Thus, we firstly study properties of transcritical flows in detail (§3.1), and then, show different aspects of subcritical flows for comparison (§3.2).

3.1. Transcritical Flows

3.1.1. Effects of Alfvén Waves

Figure 1 illustrates how the wind properties change by the effects of Alfvén waves. As for Alfvén wave,

we consider two cases of $B_0 = 3 \times 10^{14} \text{ G}$ (dotted) and $B_0 = 5 \times 10^{14} \text{ G}$ (solid). In both case the same dissipation length, $l = 10r_0$, is adopted. Wind purely driven by the neutrino heating is also shown for comparison (dashed). Since $F_{w,0} \propto B_0^3$, the input Alfvén wave energy flux of case with $B_0 = 5 \times 10^{14} \text{ G}$ is larger by a factor of 5 than that of case with $B_0 = 3 \times 10^{14} \text{ G}$. Wind structures (ρ , T , & v), entropy per baryon (S), and heating (\dot{q}_ν & \dot{q}_w) are compared in top, middle, and bottom panels, respectively.

One sees in bottom panel that the wave heating is distributed around $\sim l$ ($= 10r_0$), in contrast to the neutrino heating which is localized close to the surface. Then, the wind structures shown in top panel are modified in relatively outer region by the Alfvén waves. A clear difference is seen in velocity structure. The Alfvén waves directly accelerate the materials by wave pressure gradient and the faster winds are attained as input energy of Alfvén wave increases. Accordingly, $t_{\text{exp}} = 8.9 \times 10^{-3} \text{ s}$ in the case with larger input of Alfvén waves is much shorter than $t_{\text{exp}} = 4.4 \times 10^{-2} \text{ s}$ in the case without the waves. This indicates that the wave dissipation realizes non-equilibrium circumstances for the nuclear reactions, which encourages the r-process nucleosynthesis. Density shows more rapid decrease by the presence of the Alfvén waves to satisfy the mass conservation (eq.(2)). Temperature is also slightly lower because adiabatic cooling effectively works due to the rapid expansion (i.e. acceleration) of the plasma.

Middle panel shows that the Alfvén waves give a great influence on S in the wind. First, S is no more a constant even in the outer region where the neutrino heating is inefficient because the wave heating still occurs there. Second, S is larger except in a region closed to the surface for larger injection of Alfvén waves. This trend needs to be interpreted in detail because it is opposed to that anticipated from the neutrino heating (QW96). Variation of entropy is given by

$$\frac{dS}{dr} = \frac{m_N \dot{q}_\nu}{vT} + \frac{m_N \dot{q}_w}{vT}, \quad (16)$$

which is derived from the energy equation (4). For the neutrino heating, larger \dot{q}_ν leads to larger v and T in the winds. As a result, $\frac{\dot{q}_\nu}{vT}$ itself becomes smaller for larger \dot{q}_ν and final S is also smaller (QW96). On the other hand in the wave heating, an increase of v as a consequence of an increase of \dot{q}_w is smaller than that of \dot{q}_w itself as described below.

Based on our wave heating model, eq.(5), \dot{q}_w is pro-

portional to B_0^3 for the assumed constant initial amplitude $\delta B_0/B_0 = 0.1$. As for v , a rough dimensional estimation can be done in a following way. Without Alfvén waves, velocity, v_1 , at an arbitrary position $r = r_1$ can be derived from the Bernoulli equation (13) as

$$\frac{v_1^2}{2} + \frac{T_1 S_1}{m_N} - \frac{GM}{r_1} = -\frac{GM}{r_0} + \int_{r_0}^{r_1} dr \frac{\dot{q}_\nu}{v}, \quad (17)$$

where subscript '1' denotes physical variables at r_1 and we have used the fact that the gravitational potential term dominates at the surface, $r = r_0$. Let us assume that velocity increase to $v_1 + \Delta v_1$ by an input of Alfvén waves with energy flux, $F_{w,0}$, at r_0 . Then,

$$\begin{aligned} \frac{(v_1 + \Delta v_1)^2}{2} + \frac{(T_1 + \Delta T_1)(S_1 + \Delta S_1)}{m_N} - \frac{GM}{r_1} + \frac{F_{w,1}}{\rho_1 v_1} \\ = -\frac{GM}{r_0} + \int_{r_0}^{r_1} dr \frac{\dot{q}_\nu}{v'} + \frac{F_{w,0}}{\rho_0 v_0}, \end{aligned} \quad (18)$$

where ΔT_1 and ΔS_1 are modifications of T_1 and S_1 , and we use v' instead of v in the integral of the neutrino term because the velocity changes from that in the pure neutrino-driven wind (eq.(17)).

The wave energy converts to both kinetic energy (first term on the left of eq.18) and enthalpy (second term) of the flow. We assume that a fraction, ϵ , is transferred to the kinetic part, whereas ϵ is automatically calculated in the numerical integration to satisfy the wave energy equation (5). Comparing eqs.(17) and (18), we have

$$\frac{(v_1 + \Delta v_1)^2}{2} - \frac{v_1^2}{2} = \epsilon \left(\frac{F_{w,0}}{\rho_0 v_0} - \frac{F_{w,1}}{\rho_1 v_1} \right), \quad (19)$$

where we neglect the difference of the velocity appearing in the neutrino term. If $\Delta v_1 \ll v_1$, $\frac{\dot{q}_\nu}{v}$ in eq.(16) simply proportional to $\dot{q}_w \propto B_0^3$, hence, an increase of B_0 raises S . If $\Delta v_1 \gg v_1$, equation (19) gives $\Delta v_1 \propto \sqrt{F_{w,0}} \propto B_0^{3/2}$ for constant v_0 , provided that $\frac{F_{w,0}}{\rho_0 v_0} \gg \frac{F_{w,1}}{\rho_1 v_1}$. In the real situation v_0 has a positive correlation with B_0 so that the dependence of Δv_1 on B_0 is weaker. Therefore, $\frac{\dot{q}_\nu}{v}$ in eq.(16) is at least in proportion to $B_0^{3/2}$, showing that larger field strength directly leads to an increase of S . In the Alfvén wave-driven winds, temperature is also slightly lower due to the larger adiabatic cooling (fig.1). This effect further contributes to the increase of S as expected from eq.(16). In conclusion, Alfvén waves effectively raise

entropy in the winds to give the suitable circumstances for the r-process.

Since S varies in a region where the r-process occurs, it is not straightforwards whether the r-process criterion, eq.(14), is directly applicable. In this paper, we adopt S at $T = 0.2\text{MeV}$ as a necessary condition, based on the fact that a ratio of neutrons to seeds, a key to determine the final abundance of the r-process elements, is once fixed through the α -rich freeze-out in $T \gtrsim 0.2\text{MeV}$. The figure exhibits that $S(T = 0.2\text{MeV})$ (filled triangles) increases for larger input of the Alfvén waves. In particular, case with $B_0 = 5 \times 10^{14}\text{G}$ gives $S = 170$, which satisfies the criterion, eq.(14), for the r-process nucleosynthesis, if $Y_e \leq 0.41$.

3.1.2. Dependence on Dissipation Length

Figure 2 compares the wind properties for different dissipation lengths, $l = 5 \& 30$ but the same field strength, $B_0 = 5 \times 10^{14}\text{G}$. As illustrated in bottom panel, l controls the distribution of heating; the waves dissipate more efficiently around $\sim l$ so that the heating and acceleration (not shown) are most effective there. For smaller l , the Alfvén waves influence on the wind in an inner part; higher v , smaller ρ , and T are obtained as seen in top panel, which is consistent with the trends obtained when considering larger wave heating (§3.1.1). S is also larger in the inner region (middle panel) as the wave heating is enhanced there. However, these trends become reverse in the outer region as the wave dissipation becomes efficient for larger l case.

The wind properties in $T \gtrsim 0.2\text{MeV}$ are important with respect to the r-process nucleosynthesis, since the neutron-to-seeds ratio is determined there. Wind structure is greatly improved there in case with $l = 5$ to give smaller t_{exp} and larger S for the successful nucleosynthesis, while the modification is smaller in case with $l = 30$ as the wave dissipation occurs in farther outside. Therefore, rapid wave dissipation (short l) is favored for the r-process.

3.1.3. B_0 & l for R-process

In fig.3 we show result of the wind properties for various B_0 and l in $t_{\text{exp}}-S(T = 0.2\text{MeV})$ plane, overlayed with the r-process criterion (eq.(14)) for $Y_e = 0.4$ and 0.5 . We do not show results with $B_0 > 6 \times 10^{14}\text{G}$, because both wind velocity and Alfvén speed are approaching to the light speed, c , and our non-

relativistic treatment is not valid. (The final flow speed becomes $\simeq (0.4 - 0.5)c$ and the Alfvén speed at $r \sim 5r_0$ becomes $\simeq c$ for $B_0 = 6 \times 10^{14}\text{G}$.) The figure shows that the Alfvén waves play a role for $B_0 \gtrsim 10^{14}\text{G}$. Larger B_0 and smaller l lead to larger $S(T = 0.2\text{MeV})$ and smaller t_{exp} as described in §3.1.1 and §3.1.2. Models with $B_0 \gtrsim 5 \times 10^{14}\text{G}$ and $l \lesssim 10r_0$ satisfies the r-process condition, eq.(14), for $Y_e = 0.4$. The condition for $Y_e = 0.5$ is also satisfied with slightly larger B_0 ($= 6 \times 10^{14}\text{G}$) if $l \lesssim 10r_0$, as dependence on B_0 is sensitive.

The value, $B_0 \simeq 5 \times 10^{14}\text{G}$, can be understood by a simple energetics consideration. It is useful to introduce a plasma β value, $\beta \equiv P/(B^2/8\pi)$, a ratio of plasma pressure to magnetic pressure. Let us consider β at $r = 10r_0$:

$$(\beta_{10})^{-1} \sim 10 \left(\frac{B_0}{5 \times 10^{14}\text{G}} \right)^2 \left(\frac{0.15\text{MeV}}{T_{10}} \right)^4, \quad (20)$$

where subscript '10' denotes quantities measured at $r = 10r_0$. Here, we have used the conservation of the magnetic flux (eq.(1)) to relate B_{10} with B_0 , and we assume that the radiation pressure dominates in P . Equation (20) shows that the flow at $10r_0$ is dominated by the magnetic field energy by 10 times for $B_0 = 5 \times 10^{14}\text{G}$. Transfer of small fraction of the magnetic energy to the radiation plasma gives a great influence on the energetics and dynamics. Alfvén waves play a role in this energy transfer in our framework, and the wind properties are improved to be suitable for the r-process nucleosynthesis. Sensitive behaviors of the wind parameters on B_0 seen in fig.3 can also be interpreted by squared dependence on B_0 in eq.(20).

3.2. Subcritical Flows

We have discussed the r-process nucleosynthesis in the transcritical flows so far. This is reasonable if the plasma expands into space with much lower density. In the real situations, however, the PNS winds would be interrupted by the ejected shells existing in the outer region to form the termination shocks. If a position of the shocks are not far from the critical point, the winds might become subcritical flows eventually. Terasawa et al. (2002) pointed out that these dynamics at the outer boundary gave an influence on the r-process nucleosynthesis. Hence, it is worth studying the dynamics of the subcritical flows with Alfvén waves. In this subsection, we examine how the structures in the subcritical flows are modified compared with the transcrit-

ical case and argue possible influences on the r-process nucleosynthesis.

Infinite numbers of subcritical solutions exist for different choices of v_0 . Physically, a certain solution is selected by conditions at the outer region, such as pressure in the shell ejected by the SN explosion. The shell moves outward and the pressure would decrease as it expands. Then, it is required to treat the outer boundary in a time-dependent manner (e.g. Sumiyoshi et al. 2000) for accurate calculations. However, we construct subcritical wind structures under the steady state condition by reducing v_0 in an ad hoc way for simplicity's sake.

Figure 4 compares subcritical flows with the transcritical one for $B_0 = 5 \times 10^{14}\text{G}$ and $l = 10r_0$. As for the subcritical flows, we show cases with smaller v_0 by 0.1%(case A), 1%(B), and 2.5%(C) than that of the transcritical case. The figure shows that the wind structures in the inner region ($r \lesssim 10r_0$) are almost identical, so that t_{exp} differs only by a factor of 1.6 even between case C and the transcritical flow. Clear difference is seen in the outer region. Speed of subcritical flows in the outer region is slower, by definition, than the transcritical flow. Accordingly, the density is much higher to satisfy the mass conservation. Temperature is also higher because the wave dissipation works in the plasma heating rather than the wind acceleration. The difference in the entropy ($\propto T^3/\rho$) is small because the change of ρ is compensated by that of T , whereas the subcritical cases give slightly larger $S(T = 0.2\text{MeV})$. The r-process criterion, eq.(14), is influenced quite little as the tiny variances of S and t_{exp} further cancel out.

We would like to discuss implications on the r-process nucleosynthesis inferred from these different wind properties. The r-process nuclei are synthesized by following two sequential processes (Woosley & Hoffman 1992). In the inner region with higher temperature ($T \gtrsim 0.2\text{MeV}$), α -process proceeds to synthesize the seed nuclei with mass number, $A \sim 100$. In the outer region with lower temperature ($T \lesssim 0.2\text{MeV}$), reactions concerning charged particles cease and the neutron capture by the seed nuclei, namely the r-process in the narrow sense, dominantly occurs to produce the heavy nuclei. Since the dynamics in the inner region resemble each other, nucleosynthesis by the α -process is expected to be similar so that the neutron-to-seed ratio fixed at $T \simeq 0.2\text{MeV}$ is not different so much whether the flows are transcritical or subcritical.

A main contrast would arise in the final neutron capture in the outer region. An advantage of the subcritical flows is that the seed nuclei have the sufficient time to capture all the ambient neutrons due to the slower flow velocity (Yamada 2004). Temperature ($T \sim 0.1\text{MeV}$) of the subcritical winds is also reasonable for the neutron capture (Wanajo et al. 2002). We expect that the subcritical winds might be more favorable for the synthesis of the r-process nuclei with $A \sim 200$, whereas detailed calculation of nuclear reaction is desired to give the final conclusion.

4. Discussions

4.1. Configurations of Magnetic Fields

In this paper, we have only considered flux tubes radially open as a simplest case. If some portions of the surface are covered with closed magnetic fields, the open flux tubes expand super-radially (e.g. Goldreich & Julian 1969 for the dipole case). We can raise mainly two effects with respect to such super-radial expansions. First effect is that it reduces Alfvén speed, leading to shorter dissipation length of Alfvén waves. It may result in larger entropy due to an increase of the heating in the inner regions. Second effect is that it enhances adiabatic loss to reduce the wind speed (Suzuki 2004) and the temperature. Then, t_{exp} would be changed, whereas detailed investigation is required to tell how it is modified.

If the plasma in the closed region affects the PNS winds by magnetic reconnections, situations are quite different. The plasma in the closed regions are once heated by the wave dissipation as well as the neutrino heating and their sudden break-up leads to impulsive heating. This may also give suitable sites for the r-process nucleosynthesis as pointed out by Thompson (2003).

4.2. PNS Rotation

Massive stars are known to rotate rapidly (Tassoul 1978). Recent numerical calculations also show that the iron core is rotating prior to the collapse (Heger, Langer, & Woosley 2000; Heger, Woosley, & Spruit 2004). If the rotation is taken into account, jet-like explosion possibly takes place (Kotake, Yamada, & Sato 2003; Takiwaki et al. 2004). It is shown that such a jet-like explosion makes the products of explosive nucleosynthesis change so much (Nagataki et al. 1997, 1998; Nagataki 2000; Nagataki et al. 2003).

Although the r-process is not favored in steady, subcritical, and rigidly rotating jets in which a balance is maintained between the centrifugal and magnetic forces (Nagataki 2001), there will be still a possibility of the successful r-process nucleosynthesis in a jet-like explosion. In particular, we should investigate dynamical jets without assuming a steady state. Numerical simulations with rotation and magnetic field are highly desired to investigate such a possibility.

There will also be a possibility of the r-process nucleosynthesis in the winds on the equatorial plane. Nagataki & Kohri (2001) have investigated only steady and subcritical wind solutions which use the model of Weber & Davis (1967), although they are not relevant for the r-process. Otherwise if we investigated dynamical winds without assuming the steady-state, we may find a situation where successful r-process nucleosynthesis occurs, as pointed in Nagataki & Kohri (2001).

4.3. Possibilities of Gamma-Ray Observation

Qian, Vogel, & Wasserburg (1998; hereafter QVW98) discussed possibilities of detection of γ -ray emitted by the radioactive decay of the synthesized r-process nuclei in SN remnants (SNRs). They estimated γ -ray emissions of several isotopes with half-life, $\tau_{\text{hl}} \sim 10\text{yr}$, assuming the solar r-process abundances are explained by the accumulation of the Galactic SNe. The derived values are an order of $\sim 10^{-7}\text{\gamma cm}^{-2}\text{s}^{-1}$ if a SN explodes at a distance of 10kpc, which is below the sensitivity of International Gamma-Ray Astrophysics Laboratory (INTEGRAL), but at the level of future proposed telescope, ATHENA.

Our results indicate that magnetic PNSs could produce more r-process elements than the usual PNSs with $B_0 \sim 10^{12}\text{G}$. We would like to give a rough estimate on the γ -ray emissions from these magnetic PNS in the similar way to that adopted in QVW98. Subgroups of the NSs called anomalous X-ray pulsars (AXPs) and soft gamma repeaters (SGRs) are inferred to have strong magnetic field, $\sim 10^{14-16}\text{G}$ (Duncan & Thompson 1992; Vasisht & Gotthelf 1997; Kouveliotou et al. 1998; Zhang & Harding 2000). Although it is still premature to carry out statistical analysis on number fraction of these magnetic NSs, a rough estimate can be done. Comparison between the nearby AXPs and SNRs gives, $\lesssim 1/50$ of SNe have magnetic NSs (Guseinov et al. 2003). Arons (2003) adopted more conservative limit for birth rate of the magnetars, $10^{-5} - 10^{-3}\text{yr}^{-1}$, which indicates that 0.03 – 3%

of the SNe remain magnetic PNSs for assumed rate of SN, 0.03yr^{-1} .

Let us consider an extreme case that all the r-process elements have been synthesized by the magnetic PNSs. If we adopt 1% for the number fraction of the magnetic PNSs as a fiducial value, the required r-process yield per PNS for the solar abundance is increased by a factor of 100 against the case in which all the PNSs produce the r-process elements equally. Therefore, expected intensities of γ -ray lines from several isotopes become $\sim 10^{-5}\text{cm}^{-2}\text{s}^{-1}$ for a distance of 10kpc. Two AXPs are detected within $\sim 7\text{kpc}$ (Guseinov et al. 2003). Their field strength is derived as $\simeq 8 \times 10^{14}\text{G}$ (1E 1841-045) and $\simeq 7 \times 10^{13}\text{G}$ (1E2259+586) from the $P - \dot{P}$ diagram, whereas, these values could be larger if an effect of non-uniform rotation is taken into account (Lugones & Bobaci 2004). Unfortunately, estimated ages, $> 1000\text{yr}$, of the SNRs (Vasisht & Gotthelf 1997; Parmar et al. 1998) are much longer than the half lives ($\sim 10\text{yr}$) of the quoted nuclei in QVW98, so that it is impossible to detect the γ -ray by INTEGRAL. However, our estimate implies that γ -ray in future magnetic PNSs associated with SNe in the Galactic disk are detectable by INTEGRAL, whereas the possibility of the occurrence is low due to small birth rate ($\sim 10^{-5} - 10^{-3}\text{yr}^{-1}$).

QVW98 further considered long lived radioactive nuclei, ^{126}SN with $\tau_{\text{hl}} = 1.14 \times 10^5\text{yr}$. Their advantage is that γ -ray can be observed for a relatively longer period in spite of the weaker emissivities. Then, we do not have to wait another SN to explode. We can estimate the γ ray emission to be $\sim 2 \times 10^{-8}(\delta M/5 \times 10^{-5}M_\odot)(7\text{kpc}/d)^2\text{cm}^{-2}\text{s}^{-1}$ for 1E 1841-045 (Sanbonmatsu & Helfand 1992), and $\sim 5.5 \times 10^{-8}(\delta M/5 \times 10^{-5}M_\odot)(4\text{kpc}/d)^2\text{cm}^{-2}\text{s}^{-1}$ for 1E2259+586 (Coe & Jones 1992), where δM is the average amount of mass of a radioactive *r*-process nucleus produced in a magnetar (QVW98). Thus it will be difficult to detect γ -ray lines from these long lived radioactive nuclei by INTEGRAL. However, the γ rays from these AXPs might be marginally detectable by ATHENA whose sensitivity is $\sim 10^{-7}\text{cm}^{-2}\text{s}^{-1}$ at $E_\gamma \sim 100 - 700\text{ keV}$ in the future, whereas a large uncertainty of δM should be reduced by theoretical efforts.

4.4. Absorption Features of Supernova Spectrum

There are reports that absorption lines of Ba[II] and Ba[III] are detected in SN1987A as well as in other

Type II-P supernova in the early phase of the explosion (Mazzali et al. 1992; Mazzali & Chugai 1995), which may indicate that r-process nucleosynthesis occurred in SN1987A. Tsujimoto & Shigeyama (2001) estimated the amount of synthesized Barium in SN1987A is about $6 \times 10^{-6}M_\odot$. Thus if a SN that contains a magnetar explodes in nearby galaxies and ejected more r-process elements, the spectrum should show clearer absorption features due to Ba. In this case, Sr, $\sim 10\%$ of which is produced by the r-process (note that Sr is mostly produced by the s-process), would be observable as well (Tsujimoto & Shigeyama 2001).

5. Conclusion

We have investigated possibilities of the r-process nucleosynthesis in the PNS winds driven not only by the neutrino heating but also by the Alfvén waves. Those excited by the surface motions propagate upwardly to heat and accelerate the winds through their dissipation. As a result, larger S and smaller t_{exp} can be accomplished. We have considered the waves with initial amplitude, $\delta B_0/B_0 = 0.1$ and construct 1 dimensional spherical symmetric wind structures under the steady state condition. We have shown that field strength, $B_0 \gtrsim 5 \times 10^{14}\text{G}$, satisfies the criterion for the r-process by HW97, if the Alfvén waves dissipate around a distance, $\lesssim 10$ times of the radius, which is reasonable for the waves with period of 1ms. We also compared transcritical and subcritical flows with respect to the r-process. We have found that the final neutron captures are affected by the types of the flows, while the neutron-to-seed ratio after the α -process is expected to be similar.

Our results imply that the magnetic PNS is a more appropriate site for the r-process nucleosynthesis than PNSs with usual field strength $\sim 10^{12}\text{G}$. Based on this consideration, we have given an estimation of γ ray emissions by the radioactive nuclei from AXPs (and SGRs), relevant candidates for the magnetic NSs. Our estimates show that γ rays from the short-lived nuclei could be detected in future SNe associated with the magnetic PNSs by the present telescope, INTEGRAL, if one happens in spite of the low possibility, while those from the long-lived nuclei would be marginally detectable in the present AXPs by the future telescope, ATHENA.

We are grateful to S. Yamada, T. Murakami, D. Yonetoku, S. Wanajo, T. Kajino, and T. Shigeyama for useful discussions. Comments raised by an anonym-

mous referee have helped us quite a lot to improve the paper. This work is in part supported by a Grant-in-Aid for the 21st Century COE “Center for Diversity and Universality in Physics” at Kyoto University. T.K.S. is financially supported by the JSPS Research Fellowship for Young Scientists, grant 4607. S.N. is partially supported by Grants-in-Aid for the Scientific Research from the Ministry of Education, Science and Culture of Japan through No.S 14102004, No. 14079202 and No. 16740134.

REFERENCES

Argast, D., Samland, M., Thielemann, F.-K., Qian, Y.-Z. 2004, *A&A*, 416, 997

Arons, J. 2003, *ApJ*, 589, 871

Belcher, J. W. 1971, *ApJ*, 168, 509

Bethe H.A., Brown G.E. 1998, *ApJ*, 506, 780

Blaes, O., Blandford, R., Goldreich, P. & Madau, P. 1989, *ApJ*, 343, 839

Cardall, C.Y., Fuller, G.M. 1997, *ApJ*, 486, L111

Coe, M. J., Jones, L. R. 1992, *MNRAS*, 259, 191

Cowan J.J., Pfeiffer B., Kratz K.-L., Thielemann F.-K., Sneden C., Burles S., Tytler D., Beers T.C. 1999, *ApJ*, 521, 194

Cranmer, S. R., Field, G. B., & Kohl, J. L. 1999, *ApJ*, 518, 937

Doyle, J. G., Teriaca, L., & Banerjee, D. 1999, *A&A*, 349, 956

Duncan, R. C. & Thompson, C. 1992, *ApJ*, 392, L9

Epstein, R. I. 1979, *MNRAS*, 188, 305

Freiburghaus C., Rosswog S., and Thielemann F.-K. 1999, *ApJ*, 525, L121

Goldreich, P. & Julian, W. H. 1969, *ApJ*, 157, 869

Goldstein, M. L. *ApJ*, 1978, 219, 700

Goodman, J., Dar, A., & Nussinov, S. 1987, *ApJ*, 314, L7

Guseinov, O. H., Yazgan, E., & Ankay, A. 2003, *Int. J. Mod. Phys. D*, 12, 1

Heger, A., Langer, N., & Woosley, S. E. 2000, *ApJ*, 528, 368

Heger, A., Woosley, S. E., & Spruit, H. C. 2004, *astro-ph/0409422*

Heyvaerts, J. & Priest, E. R. 1983, *A&A*, 117, 220

Hoffman, R. D., Woosley, S. E., & Qian, Y.-Z. 1997, *ApJ*, 482, 951 (HWQ94)

Hollweg, J. V. 1982, *ApJ*, 254, 806

Ishimaru Y. & Wanajo S. 1999, *ApJ*, 511, L33

Jacques, S. A. 1977, *ApJ*, 215, 942

Keil, W., Janka, H.-Th., & Müller, E. 1996, *ApJ*, 473, L111

Kojima, Y. & Okita, T. 2004, *ApJ*, 614, 922

Kotake, K., Yamada, S., Sato, K. 2003, *ApJ*, 595, 304

Kouveliotou, C. et al. 1998, *Nature*, 393, 235

Lamers, H. J. G. L. M. & Cassinelli, J. P. 1999, ‘Introduction to Stellar Wind’, Cambridge

Lugones, G. & Bobaci, I. 2004, *Phys. Rev. Lett.*, submitted (*astro-ph/0411507*)

Mazzali, P.A., Lucy, L.B., Butler, K. 1992, *A&A*, 258, 399

Mazzali, P.A. & Chugai, N.N. 1995, *A&A*, 303, 118

McWilliam A., Preston G.W., Sneden C., Searle L. 1991, *AJ*, 109, 2757

Meyer B.S. 1995, *ApJ*, 449, L55

Nagataki, S., Hashimoto, M., Sato, K., & Yamada, S. 1997, *ApJ*, 486, 1026

Nagataki, S., Hashimoto, M., Sato, K., Yamada, S., & Mochizuki, Y.S. 1998, *ApJ*, 492, L45

Nagataki, S., 2000, *ApJS*, 127, 141

Nagataki, S. 2001, *ApJ*, 551, 429

Nagataki, S. & Kohri, K. 2001, *PASJ*, 53, 547

Nagataki, S., Mizuta, A., Yamada, S., Takabe, H., & Sato, K., 2003, *ApJ*, 596, 401

Otsuki K., Tagoshi H., Kajino T., & Wanajo S. 2000, *ApJ*, 533, 424

Parmar, A. N., Oosterboek, T., Favata, F., Pightling, S., Coe, M. J., Mereghetti, S., Israel, G. L. 1998, *A&A*, 330, 175

Qian Y.-Z. & Woosley S.E. 1996, *ApJ*, 471, 331 (QW96)

Qian, Y. Z., Vogel, P., & Wasserburg, G. J. 1998, *ApJ*, 506, 868 (QVW98)

Rosswog, S., Davies, M.B., Thielemann, F.-K., & Piran, T. 2000, *A&A*, 369, 171

Sanbonmatsu, K. Y. & Helfand, D. J., 1992, *AJ*, 104, 2189

Sumiyoshi, K., Suzuki, H., Otsuki, K., Terasawa, M., & Yamada, S. 2000, *PASJ*, 52, 601

Suzuki, T. K. 2004, *MNRAS*, 349, 1227

Takahashi K., Witti J., & Janaka H.-Th. 1994, *A&A*, 286, 857

Takiwaki, T., Kotake, K., Nagataki, S., & Sato, K. 2004, *ApJ*, in press.

Tassoul, J.-L., 1978, *Theory of Rotating Stars* (Princeton: Princeton Univ. Press)

Terasawa, M., Sumiyoshi, K., Yamada, S., Suzuki, H., & Kajino, T. 2002, *ApJ*, 578, L137

Thompson. C. & Duncan, R. C. 1996, *ApJ*, 473, 322

Thompson, C., Lyutikov, M. & Kulkarni, S. R. 2002, *ApJ*, 574, 332

Thompson, T. A., Burrows, A. & Meyer, B. S. 2001, *ApJ*, 562, 887

Thompson, T. A. 2003, *ApJ*, 585, L33

Tsujimoto, T., Shigeyama, T. & Yoshii, Y. 1999, *ApJ*, 519, L63

Tsujimoto, T. & Shigeyama, T. 2001, *ApJ*, 561, L97

Tubbs, D.L., Schramm, D.N. 1975, *ApJ*, 201, 467

van den Bergh S. & Tamman G.A., 1991, *ARA&A*, 29, 363

van den Heuvel E. & Lorimer D. 1996, *MNRAS*, 283, L37

Vasisht, G. & Gotthelf, E. V. 1997, *ApJ*, 486, L129

Wanajo, S., Kajino, T., Mathews, G., & Otsuki, K. 2001, *ApJ*, 554, 578

Wanajo, S., Itoh, N., Ishimaru, Y., Nozawa, S., Beers, T. C. 2002, *ApJ*, 577, 853

Wanajo, S., Tamamura, M., Itoh, N., Nomoto, K., Ishimaru, Y., Beers, T. C., Nozawa, S. 2003, *ApJ*, 593, 968

Weber, E.J. & Davis, L. 1967, *ApJ*, 148, 217

Williams, R. E. 1987, *ApJ*, 320, L117

Wiringa R. B., Fiks U., & Fabrocini A. 1988, *Phys. Rev. C*, 38, 1010

Woosley, S. E. & Hoffman, R. D. 1992, *ApJ*, 202

Woosley S.E., Wilson J.R., Mathews G.J., Hoffman R.D., & Meyer B.S. 1994, *ApJ*, 433, 229

Yamada, S. 2004, private communication

Zhang, B. & Harding, A. K. 2000, *ApJ*, 535, L51

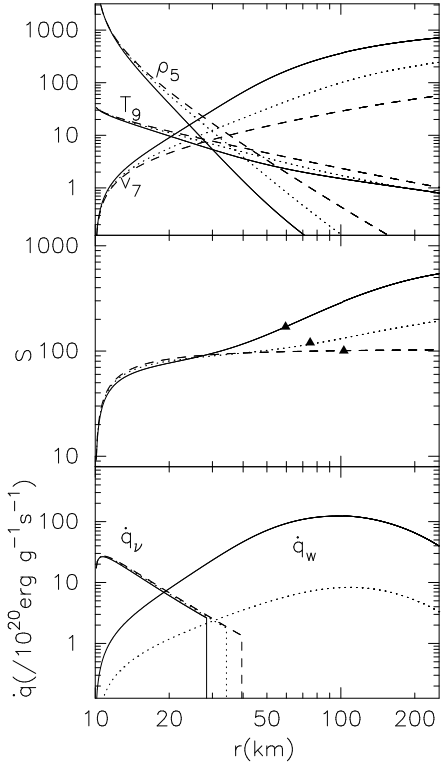


Fig. 1.— Properties of Alfvén wave-driven winds for $B_0 = 5 \times 10^{14}$ G (solid) and 3×10^{14} G (dotted). Dissipation length is set to be $l = 10r_0$ for both cases. Result of neutrino driven-wind (without Alfvén waves) is also displayed for comparison (dashed). *top* : Comparison of density in 10^5 g cm $^{-3}$, temperature in 10^9 K, and velocity in 10^7 cm s $^{-1}$. *middle* : Comparison of entropy per baryon in unit of k_B . Triangles indicate positions where $T = 0.2$ MeV. *bottom* Comparison of heating (10^{20} erg/g s) by the neutrino (\dot{q}_ν) and wave dissipation (\dot{q}_w).

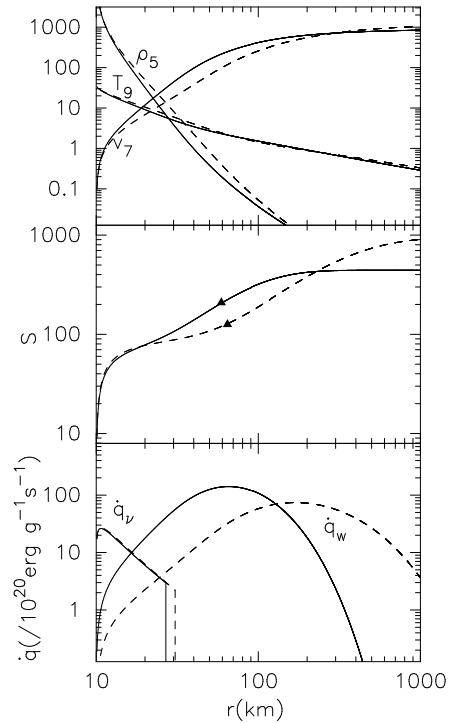


Fig. 2.— Comparison of the wind properties for different dissipation lengths, $l = 5$ & $30 \times r_0$ but the same $B_0 = 5 \times 10^{14}$ G. Each panel is the same as in fig.1 but the horizontal and vertical scales are different.

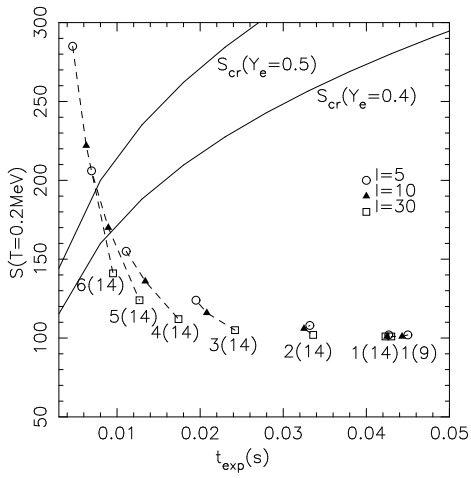


Fig. 3.— $t_{\text{exp}}(\text{s})$ (X-axis) and S at $T = 0.2\text{MeV}$ (Y-axis) for various parameters of Alfvén waves. Open circles, filled triangles, and open squares are results with $l = 5, 10, \& 30$, respectively. Numbers denote magnetic field strength at the surface. For example 6(14) indicates $B_0 = 6 \times 10^{14}\text{G}$. Results with the same B_0 are connected by dashed lines. Solid lines are the conditions for the r-process by HWQ97 (eq.14) for $Y_e = 0.4 \& 0.5$.

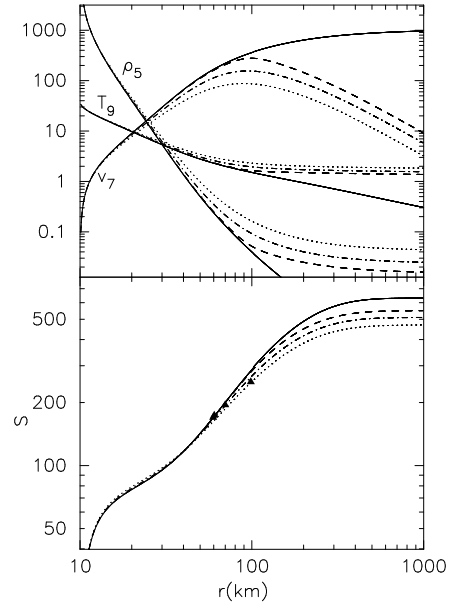


Fig. 4.— Wind properties of subcritical flows in comparison with transonic flow (solid) for $B_0 = 5 \times 10^{14}\text{G}$ and $l = 10r_0$. Dashed, dot-dashed, and dotted lines are cases with reducing v_0 by 0.1%, 1%, & 2.5%, respectively. Upper and lower panels are the same as in top and middle panels in fig.1, but the horizontal and vertical scales are different.